Korean J. Chem. Eng., **30**(3), 714-723 (2013)
DOI: 10.1007/s11814-012-0194-x

Adsorption of phenol and 1-naphthol onto XC-72 carbon

Liming Zuo, Shaoming Yu†, Leilei Cheng, and Erling Du

School of Chemical Engineering, Hefei University of Technology and Anhui Key Laboratory of Controllable Chemical Reaction & Material Chemical Engineering, Hefei 230009, Anhui, China
(*Received 4 July 2012 • accepted 5 November 2012*)

Abstract−XC-72 carbon (XC-72) was characterized by SEM, XPS, N_2 adsorption-desorption, particle size distribution analysis and potentiometric acid-base titration. The adsorption of phenol and 1-naphthol on XC-72 was studied as a function of contact time, pH, adsorbent content and temperature. The kinetic adsorption data were described well by the pseudo-second-order model. The adsorption isotherms of phenol were described well by Freundlich model, while the adsorption isotherms of 1-naphthol were fitted well by Langmuir model. The results demonstrated that XC-72 had much higher adsorption capacity for 1-naphthol than for phenol. The adsorption thermodynamic data were calculated from the temperature-dependent adsorption isotherms at T=293, 313 and 333 K, and the results indicated that the adsorption of phenol was an exothermic process, whereas the adsorption of 1-naphthol was an endothermic process. XC-72 is a suitable material for the preconcentration of phenol and 1-naphthol from large volumes of aqueous solutions.

Key words: XC-72 Carbon, Adsorption, Phenol, 1-Naphthol, Kinetics

INTRODUCTION

Phenolic compounds are common contaminants in wastewater due to their wide use in industrial activities such as the petrochemical industries, Kraft pulp mills, olive oil production, and other chemical industries [1]. Since phenols are harmful to organisms even at low concentrations and difficult to degrade biologically, many of them have been classified as priority pollutants in wastewater by the European Union, and the 80/778/EC directive lays down a maximum concentration of 0.5 μg/L for total concentrations of phenols in drinking water [2]. Therefore, it is required to eliminate phenols from wastewater before it is discharged to the natural environment.

There are many methods for the removal of phenols from aqueous solutions such as oxidation, ion exchange, adsorption, solvent extraction [3-7]. Compared to other methods, adsorption is widely used for water treatment due to its sludge-free clean operation, economics, availability of wide range of adsorbents and complete removal of phenols from wastewaters [8-11].

Carbon black (CB), an important chemical material, is the accepted generic name for a group of chemically heterogeneous, carbonaceous materials produced during the incomplete combustion of biomass and fossil fuels or weathering of graphitic carbon in rocks [12]. In recent years, CB has aroused wide attention as an effcient adsorbent in industrial wastewater treatment due to its unique structure and intrinsic surface properties [13]. XC-72 is a kind of carbon black nanoparticle. It has been used in the preparation of catalyst [14] and as adsorbent in the removal of heavy metal ions [15]. XC-72 has high surface area and defected sites, which indicates that it possesses high adsorption capacity in the removal of organic and inorganic pollutants from the large volumes of aqueous solutions [15]. In this work, the adsorption of phenol and 1-naphthol as two typical phenols on XC-72 was investigated by batch technique with respect to the contact time, adsorbent content, pH and temperature. The adsorption mechanism was discussed in detail according to the experimental results.

†To whom correspondence should be addressed.
E-mail: shmyu@hfut.edu.cn

MATERIALS AND METHODS

1. Chemicals

All chemicals used in the experiments were purchased in analytical purity and used without any purification. XC-72 was obtained from Cabot Corporation (USA) and used as received without further purification. Phenol and 1-naphthol were purchased from Sinopharm Chemical Reagent Corporation (China).

2. Characterization of the Sorbent

XC-72 was characterized by scanning electron microscope (SEM), X-ray photoelectron spectroscopy (XPS), N_2 adsorption-desorption, particle size distribution (PSD), and potentiometric acid-base titration in detail. The morphology was characterized by a field emission SEM (FE-SEM, JEOL JSM-6700, Tokyo, Japan). The XPS measurement was performed on a Thermo VG ESCALAB 250 spectrometer equipped with an Al Kα ($h\nu$=1486.6 eV) source. The surface charging effects were corrected with C 1s peak at 284.4 eV as a reference. N_2 adsorption-desorption isotherms were obtained using a Tristar II 3020 automatic surface area and pore analyzer. The sample was degassed in the analysis port at 300 °C for 4 h in vacuum. The adsorption data were then employed to determine surface area using the Brunauer Emmett and Teller (BET). The pore size of XC-72 was determined by the Barrett-Joyner-Halenda (BJH) method. The PSD analysis was performed with laser particle size analyzers (MS-2000, Malvern Co., UK). The solid content of dispersive suspensions was adjusted to be 0.4 g/L, which is according to the value of experimental sorbent content. The potentiometric acid-base titrations were performed at 293±1 K with a Mettler Toledo DL50 titration apparatus (equipped with a combined electrode) under argon atmo-

sphere, using NaOH as titration solution. The electrode was calibrated in pH 4.00, 6.86, 9.18 buffers (Alfa Aesar). Before the titration, the suspensions were titrated up to pH ~3 and purged with argon gas for about 1 h. Then the titration was carried out at pH value from 3 to 11 by using 0.08389 mol/L NaOH. The equilibrium value was taken when showing a drift less than 0.03 mV per second [16, 17].

3. Adsorption Experiments

All adsorption experiments were carried out under ambient conditions by using batch technique in polyethylene centrifuge tubes. The pH values of the systems were adjusted by adding negligible volumes of 0.01 or 0.1 mol/L $HClO_4$ or NaOH to achieve the desired pH values. The test tubes were shaken for 24 h at desired pH and temperature to achieve the adsorption equilibration and then centrifuged at 9,000 rpm for 30 min to separate the solid from liquid phases. The concentrations of phenols in the supernatants were determined by UV-vis spectrophotometer at the appropriate optimum UV wavelengths of 235 and 245 nm for phenol and 1-naphthol, respectively.

The adsorption percent (%) of phenol and 1-naphthol on XC-72 was calculated from the difference between the initial concentration (C_0) and the final one (C_e) in the supernatant after centrifugation:

$$\text{Adsorption } \% = \frac{C_o - C_e}{C_o} \times 100\% \quad (1)$$

The amount of phenol and 1-naphthol adsorbed on the solid phase (q_e, mg/g) was calculated from C_0, C_e, the volume of the suspension (V, mL) and the mass of the adsorbent (m, g):

$$q_e = \frac{C_o - C_e}{m} \times V \quad (2)$$

All experimental data were the averages of duplicate or triplicate experiments. The relative errors of the data were about 5%.

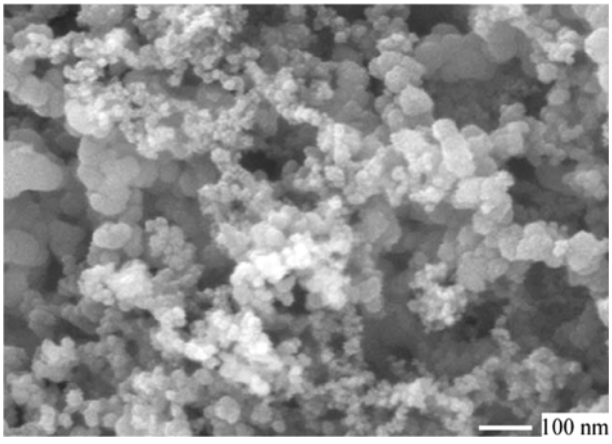

Fig. 1. SEM image of XC-72.

RESULTS AND DISCUSSION

1. Sorbent Characteristics

The SEM image (Fig. 1) shows that XC-72 particles are spherical with a diameter range of 5-50 nm. Due to inter-molecular force, the isolated XC-72 particles of different sizes can form a grape-like aggregated structure.

XPS technique is a surface-sensitive method which provides the surface functional groups of XC-72. Fig. 2(a) and Table 1 show the content of contained elements in XC-72. From them, one can see that XC-72 contains more than 90% elemental carbon, with oxygen as the other major constituent. The high resolution O 1s XPS spectrum (Fig. 2(b)) can be fitted by convoluting three individual peaks: 1) the peak at 532.0±0.2 eV corresponds to carbonyl functional groups (C=O); 2) the peak at 533.2±0.2 eV corresponds to

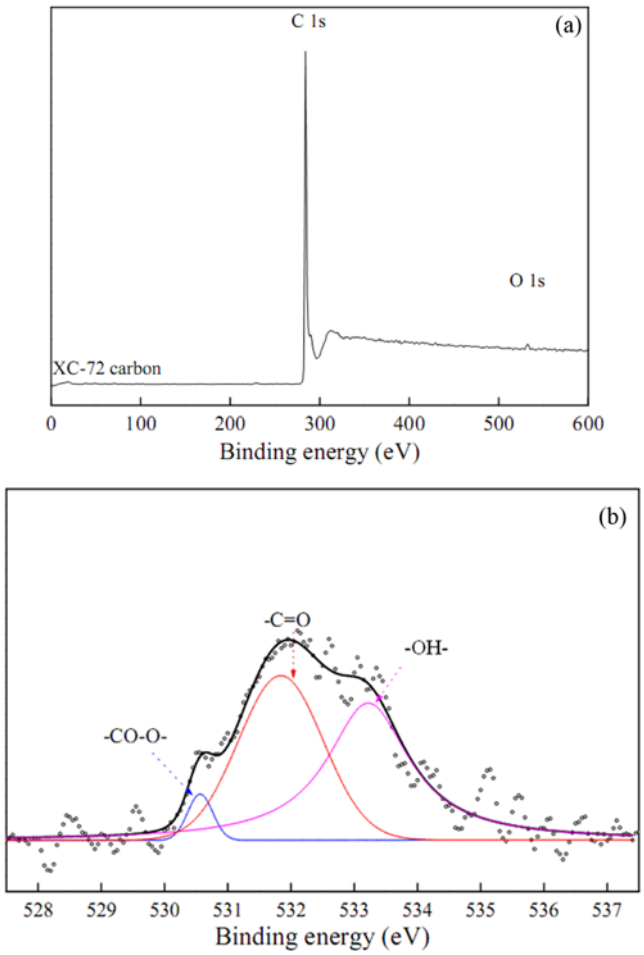

Fig. 2. XPS wide-scan (a), O 1s high-resolution (b) spectrum of XC-72.

Table 1. XPS spectra of XC-72

	Name	Peak BE (eV)	Height counts	FWHM (eV)	Area (P) CPS. (eV)	At%
XC-72	C1s	284.4	126406.74	0.87	171517.64	98.46
	O1s	532.1	1291.75	2.45	3910.58	0.96
	N1s	400.6	293.54	0.23	654.41	0.24
	S2p	163.7	614.58	0.89	1347.77	0.34

hydroxyl functional groups (-OH); and 3) the peak at 530.6±0.2 eV corresponds to carboxyl functional groups (-CO-O-) [18-20]. Therefore, oxygen-containing functional groups are present on the surfaces of XC-72.

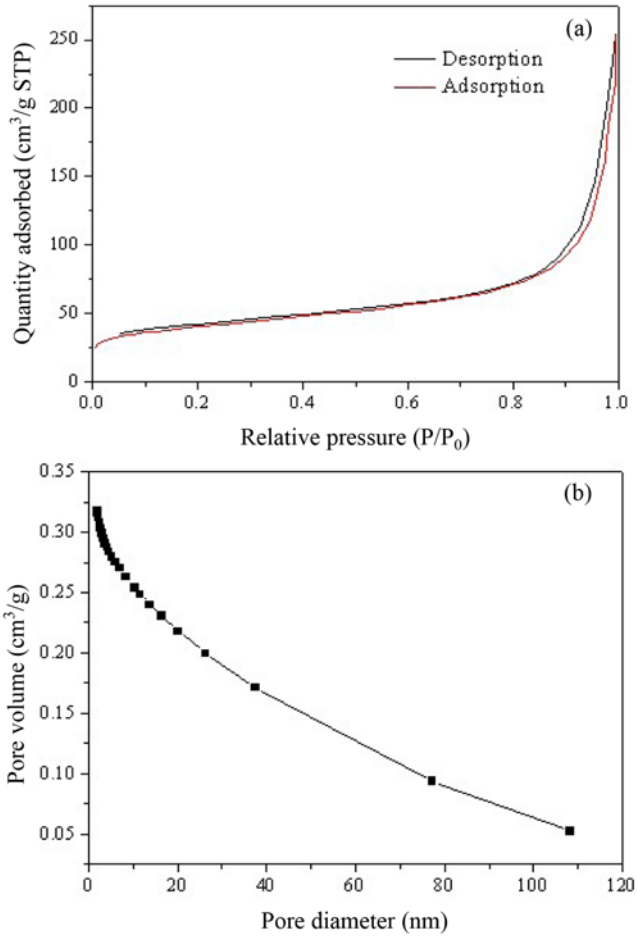

Fig. 3. N_2 adsorption–desorption isotherm (a) and corresponding BJH pore size distribution curve (b) of XC-72, the pore-size distribution was calculated from the desorption branch of the isotherm.

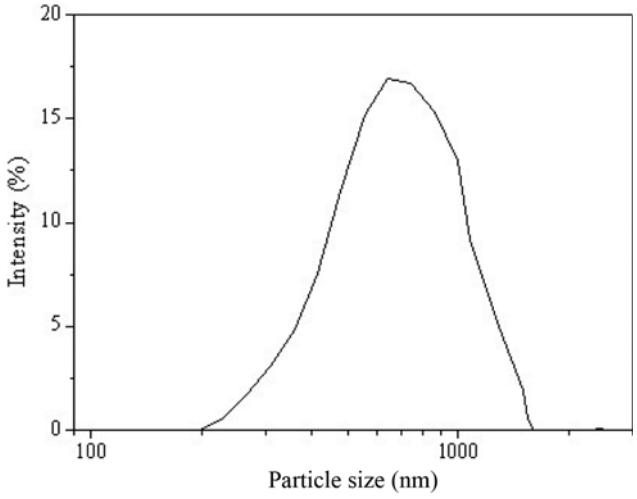

Fig. 4. Particle size distribution of XC-72.

N_2 adsorption-desorption isotherms and corresponding BJH pore-size distribution curve of XC-72 are shown in Fig. 3. The average pore size for XC-72 is 13.12 nm with a wide distribution of pore size. The BET surface area and corresponding pore volume of XC-72 are 141.1 m^2/g and 0.2505 cm^3/g, respectively.

Results of the particle size distribution analysis show that the XC-72 particles are a mixture of small particles with diameters of 200-

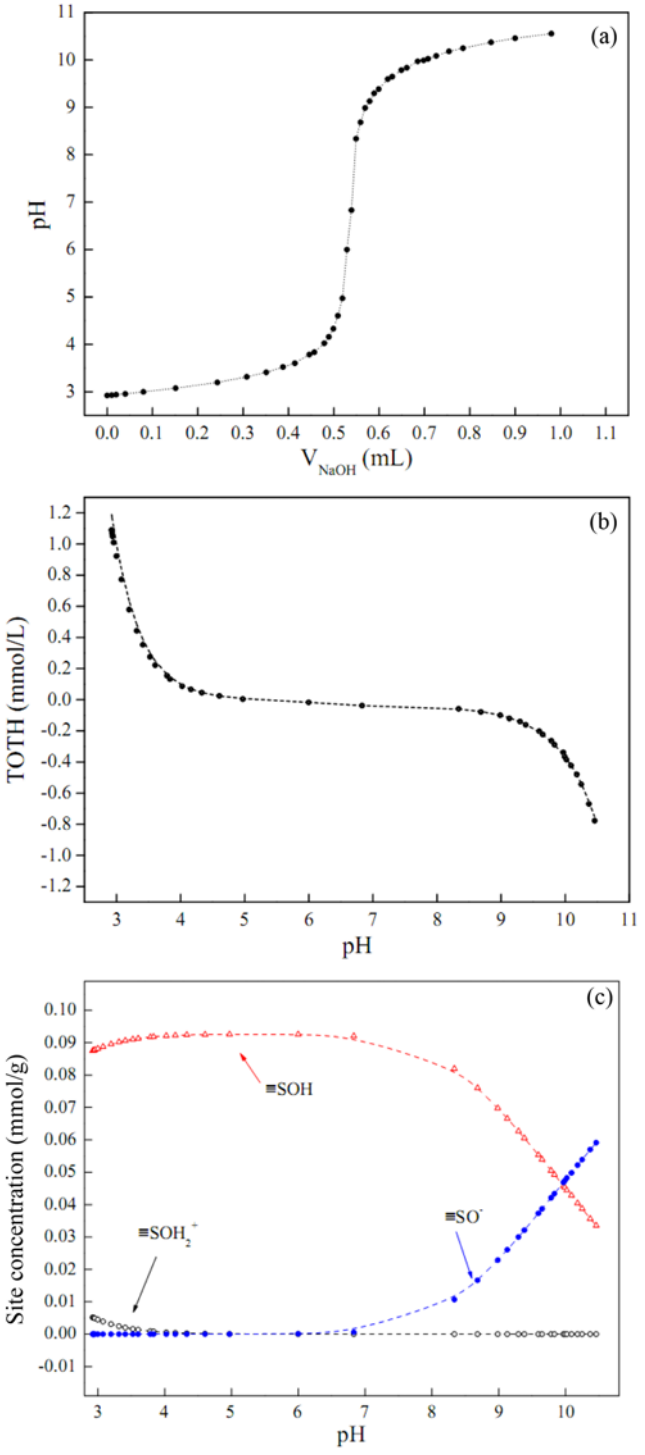

Fig. 5. Potentiometric titration curve (a), TOTH curve (b), and distribution of species (c) of XC-72. Mass content (m/V): 0.4 g/L, T=293±1 K.

1,100 nm. The average diameter is around 705 nm (Fig. 4). The distribution curve shows a log normal shape. There is a formation of particle aggregation for single XC-72 particles in aqueous solutions due to the inter-molecular force among the XC-72 particles and the presence of amounts of hydrophobic groups on the particle surface.

Potentiometric acid-base titration is an effective technique to study adsorbent surface properties (such as proton surface charge density) in aqueous solution [21,22]. The surface properties of XC-72 were characterized using acid-base titration. TOTH, the total concentration of consumed protons in the titration process, is calculated from the following equation:

$$TOTH = \frac{-(V_b - V_{e1}) \times C_b}{V_0 + V_{at} + V_b} \quad (3)$$

where V_0 represents the initial volume of the suspension, V_b and V_{eb1} are the volume of NaOH added at the different titration points and that of NaOH used in the titration at the Gran point to zero on the acidic side, C_b is the concentration of NaOH used in the titration process.

Assuming that surface sites (SOH) are amphoteric, i.e., can either be protonated to form (SOH_2^+) or deprotonated to form (SO^-). The concentration of protonated and deprotonated sites can be estimated from acid-base titration [23,24]. The protonation and deprotonation reactions are expressed as:

$$\equiv SOH + H^+ \Leftrightarrow \equiv SOH_2^+ \quad (4)$$

$$\equiv SOH \Leftrightarrow \equiv SO^- + H^+ \quad (5)$$

Fig. 5(a) shows the titration curve of pH vs. volume of NaOH used in the titration process. The titration data are modeled by the constant capacitance model (CCM). The titration curve of TOTH vs. pH is shown in Fig. 5(b). The solid line expresses the result simulated by FITEQL 3.1 code. The distribution of surface site concentration of XC-72 calculated from titration curve with the aid of FITEQL 3.1 as a function of pH is shown in Fig. 5(c). As shown in Table 2, the intrinsic acidity constants of SOH sites of XC-72 are optimized to be $\log K_{a1}$=2.46 for $\equiv SOH_2^+$ ($\equiv SOH + H^+ \leftrightarrow \equiv SOH_2^+$) and $\log K_{a2}$= −7.90 for SO^- ($\equiv SOH \leftrightarrow \equiv SO^- + H^+$), respectively. As shown in Fig. 5(c), it is clear that the site (SO^-) concentration increases with increasing pH, whereas the sites ($\equiv SOH$, $\equiv SOH_2^+$) concentration decreases with increasing pH. K_{a1} and K_{a2} are linked together by the following equation: $((|\log K_{a1}| + |\log K_{a2}|)/2 = pH_{pzc})$ [16]. The surface site concentration of XC-72 from the acid-base titration is calculated to be 9.27×10^{-5} mol/g. The value of the point of zero charge (pH_{pzc}) of XC-72 is calculated to be 5.18.

Table 2. Intrinsic acidity constants and site concentrations simulated by the 1-site model for XC-72

		XC-72
logK	$\equiv SOH + H^+ \leftrightarrow SOH_2^+$	2.46
	$\equiv SOH - H^+ \leftrightarrow \equiv SO^-$	−7.90
C (mol/g)		9.27×10^{-5}

2. Adsorption Kinetics

Fig. 6 shows the adsorption kinetics of phenol and 1-naphthol on XC-72. The adsorption of phenol and 1-naphthol on XC-72 was very fast: 3 and 4 h of contact were enough to achieve the adsorption equilibrium phenol and 1-naphthol to achieve equilibrium, respectively. From the kinetic adsorption data, the shaking time was fixed to 24 h to ensure the adsorption equilibrium for the following experiments. The pseudo-second-order model was applied to simulate the kinetic adsorption. The pseudo-second-order model consists of all the steps of adsorption including external film diffusion, adsorption, and internal particle diffusion, which can be written as [25,26]:

$$\frac{dq_t}{dt} = k_2(q_e - q_t)^2 \quad (6)$$

where k_2 [g/(mg·min)] is the rate constant of the pseudo-second order adsorption, q_e and q_t are the adsorbed phenols (mg/g) at equilibrium and at time t (min), respectively. The initial adsorption rate v_0 [mg/(g·min)] is calculated as:

$$v_0 = k_2 q_e^2 \quad (7)$$

Eq. (6) can be rearranged to give the linear expression:

$$\frac{t}{q_t} = \frac{1}{v_0} + \frac{1}{q_e} t \quad (8)$$

Thus the values of v_0 and k_2 can be determined by plotting t/q_t

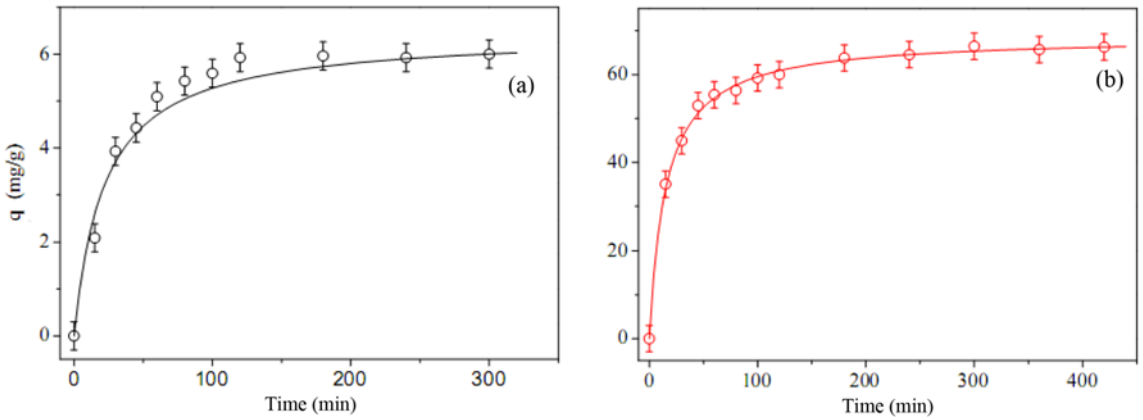

Fig. 6. Adsorption kinetics of phenol (a) and 1-naphthol (b) on XC-72. Lines represent the model fitting of pseudo-second-order equation. C(Phenol)initial=8 mg/L, C(1-naphthol)initial=32 mg/L, T=293±1 K, m/V(Phenol)=0.4 g/L, m/V(1-naphthol)=0.4 g/L, pH=7.0±0.1.

Table 3. Kinetic parameters of pseudo-second-order model fitting for phenol and 1-naphthol adsorption on XC-72

Phenols	V_0 [mg/(g·min)]	q_e (mg/g)	R^2
Phenol	0.2899	6.45	0.99
1-Naphthol	4.4691	68.68	0.99

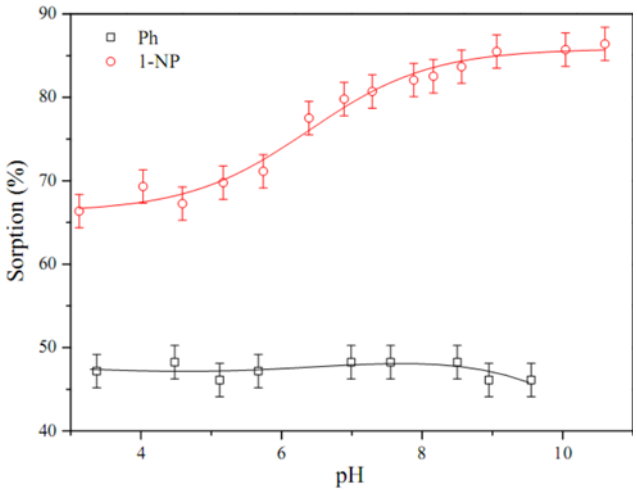

Fig. 7. Adsorption of phenol and 1-naphthol as a function of pH values. C(Phenol)initial=8 mg/L, C(1-naphthol)initial=32 mg/L, T=293±1 K, m/V(Phenol)=0.4 g/L, m/V(1-naphthol)=0.4 g/L.

versus t and extracting information from the least-squares analysis of slope and intercept and substituting into Eq. (8). The kinetic parameters of pseudo-second-order model fitting for phenol and 1-naphthol adsorption on XC-72 are listed in Table 3. The correlation coefficients of the pseudo-second-order rate equation for phenol and 1-naphthol are very close to 1, which suggests that the kinetic adsorption of phenol and 1-naphthol on XC-72 can be well described by the pseudo-second-order rate model.

3. Effect of pH

pH is an important parameter controlling the adsorption process. Fig. 7 shows the effect of pH on the adsorption of phenol and 1-naphthol on XC-72. The adsorption of phenol has no obvious variations at pH range of 3-8 and decreases at pH>8, whereas the adsorption of 1-naphthol increases slowly with pH increasing from 3 to 11 and then maintains the high level with increasing pH. The results are consistent with the adsorption of phenol on modified rectorite and 2-naphthol on carbon nanotubes [27,28], where the adsorption of phenol decreased with increasing pH at high pH values and adsorption of 2-naphthol on carbon nanotubes increased with pH even at the pH values higher than pKa.

The adsorption process may be influenced both by the adsorbent surface functionality and by the specific electronic properties of the adsorbate functional groups. From the results of potentiometric acid-base titration, it can be inferred that the distribution of surface site species of XC-72 changes with different pH values. At $pH<pH_{pzc}$, the protonated site ($\equiv SOH_2^+$) dominates and the surface charge of the adsorbent is positive. With increasing pH, the concentration of the protonated site ($\equiv SOH_2^+$) decreases while that of the deprotonated site ($\equiv SO^-$) increases. Phenol and 1-naphthol are weak acid compounds and would be dissociated at $pH>pK_a$ (pK_a=9.92 for phenol and 9.34 for 1-naphthol). The content of nondissociated and dissociated species can be calculated according to the following equations [29,30]:

$$f_N=(1+10^{pH-pK_a})^{-1} \quad (9)$$

$$f=(1+10^{pK_a-pH})^{-1} \quad (10)$$

where f_N and f represent the content of nondissociated and dissoci-

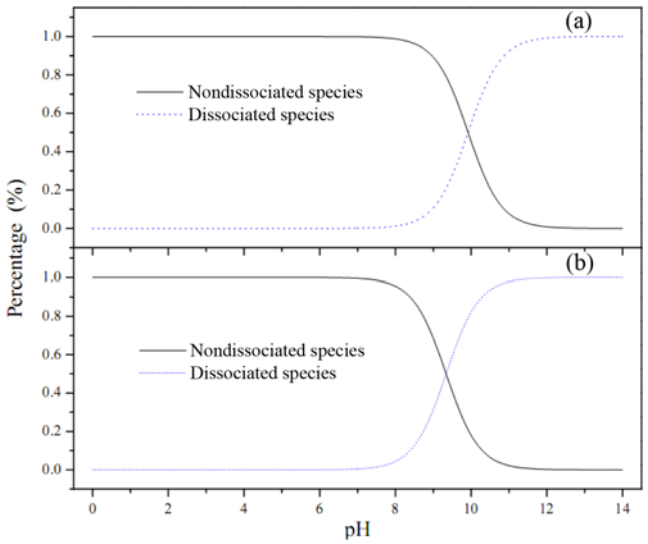

Fig. 8. Species distribution of phenol (a) and 1-naphthol (b) as a function of pH values.

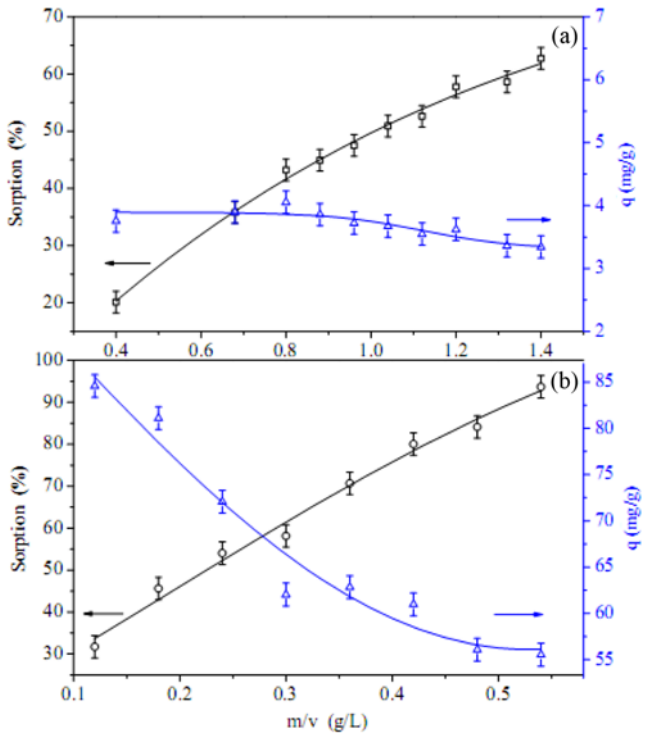

Fig. 9. Adsorption of phenol (a) and 1-naphthol (b) as a function of XC-72 content. C(Phenol)initial=8 mg/L, C(1-naphthol) initial=32 mg/L, T=293±1 K, pH=7.0±0.1.

ated species, respectively. Fig. 8 demonstrates the distribution of nondissociated or dissociated species for phenol and 1-naphthol. Phenols are present in neutral form when pH is about 2 units lower than pK_a [31]. When in alkaline solution, phenols are in a negative ionic form and the surface of XC-72 is negatively charged, which does not favor adsorption because of the repulsive force between the phenolate ion and negative charge of the surface of XC-72 [32]. The adsorption of phenol trends to decline when pH is close to 8; however, the adsorption of 1-naphthol maintains level. The inverse result suggests that there must be a certain specific adsorption-enhancement interaction to counterbalance the repulsive force. It may be attributed to the difference of the structure and properties between phenol and 1-naphthol. As we know, 1-naphthol possess one more benzene ring than phenol; therefore, the π-π dispersion force between the aromatic ring of 1-naphthol and XC-72 would be much higher than that between phenol and XC-72, which is probably the reason why adsorption of 1-naphthol maintains a high level at pH> pK_a [30]. Chen et al. [33] have reported that the strong adsorptive interaction between hydroxyl-substituted aromatics and carbon nanotubes was mainly due to the electron-donating effect of the hydroxyl group, which caused a strong electron-donor-acceptor (EDA) interaction between the adsorbates and the π-electron-depleted regions

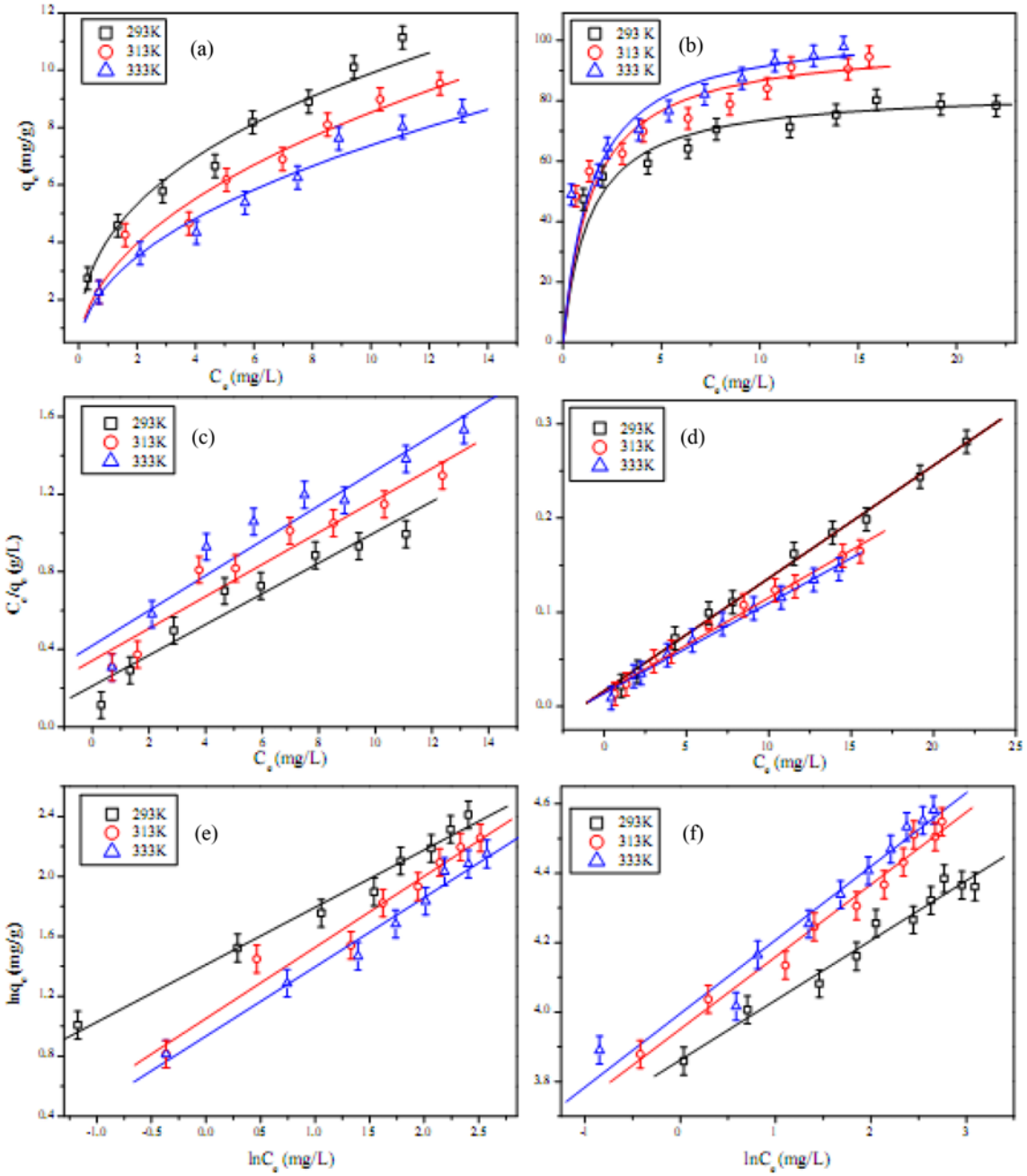

Fig. 10. Adsorption isotherms of phenol (a) and 1-naphthol (b), fitting lines of the Langmuir adsorption isotherms of phenol (c) and 1-naphthol (d) and fitting lines of the Freundlich adsorption isotherms of phenol (e) and 1-naphthol (f) at three different temperatures. m/V(Phenol)=0.4 g/L, m/V(1-naphthol)=0.4 g/L, pH=7.0±0.1.

on the grapheme surfaces of carbon nanotubes. The surface functional groups and surface properties are quite important for the removal of organic pollutants from aqueous solutions [20,34].

4. Effect of Adsorbent Content

Fig. 9 shows the effect of XC-72 content on the removal of phenol and 1-naphthol. The adsorption percent of the two phenols increases with increasing adsorbent mass. However, the adsorption capacity decreases with increasing adsorbent content. The decrease in concentration of phenols adsorbed (q_e) on XC-72 with increasing adsorbent mass is due to the split in the flux, or the concentration gradient between solute concentration in the solution and the solute concentration on the solid surfaces. Thereby, with increasing adsorbent mass, the amount of phenols adsorbed onto unit weight of adsorbent gets split, therefore causing a decrease in q_e value with increasing adsorbent mass content [35-37].

5. Adsorption Isotherms

Fig. 10 presents the adsorption isotherms of phenol and 1-naphthol on XC-72 obtained at 293, 313 and 333 K. Both the Langmuir and the Freundlich models were employed to fit the experimental adsorption data. The Langmuir isotherm can be represented by the following equation [38]:

$$q_e = \frac{bq_{max}C_e}{1+bC_e} \quad (11)$$

where q_{max} (mg/g) and b ($L \cdot mg^{-1}$) are Langmuir constants related to adsorption capacity and adsorption energy, respectively.

The Freundlich isotherm model has the following form:

$$q_e = k_F C_e^n \quad (12)$$

where k_F ($mg^{1-n} \cdot L^n/g$) represents the adsorption capacity when adsorbate equilibrium concentration equals to 1, and n represents the degree of adsorption dependence at equilibrium concentration.

The Langmuir and Freundlich constants obtained by fitting the adsorption equilibrium data are listed in Table 4. The experimental data of phenol and 1-naphthol can be fit well by both Langmuir and Freundlich models, which means physical adsorption has occurred [33,39,40]. In contrast, the Freundlich model fits the adsorption data of phenol better than the Langmuir model, while the Langmuir model fits the adsorption data of 1-naphthol better. It can be known from Table 4 that '1/n' values are less than unity, indicating that phenol molecules are favorably adsorbed by XC-72 at all temperatures [41, 42]. XC-72 has nonlinear adsorption isotherms for phenol and 1-naphthol because of the heterogeneous adsorption sites of XC-72.

6. Adsorption Thermodynamics

Temperature is an important parameter that dominates the physicochemical behavior of organics in the environment. The thermodynamic parameters (ΔG^o, ΔS^o and ΔH^o) of phenol and 1-naphthol adsorption on XC-72 are calculated from the temperature-dependent adsorption isotherms. The parameters are useful in defining whether the adsorption reaction is endothermic or exothermic, and the spontaneity of the adsorption process. The free energy change (ΔG^o) is calculated by the following equation:

$$\Delta G^o = -RT \ln K^o \quad (13)$$

where R [8.314 J/(mol·K)] is the ideal gas constant, T (K) is the temperature in Kelvin, and K^o is the adsorption equilibrium constant. Values of $\ln K^o$ are achieved by plotting $\ln K_d$ vs. C_{eq} and extrapolating C_{eq} to zero, the value of intercept is $\ln K^o$ value (Fig. 11).

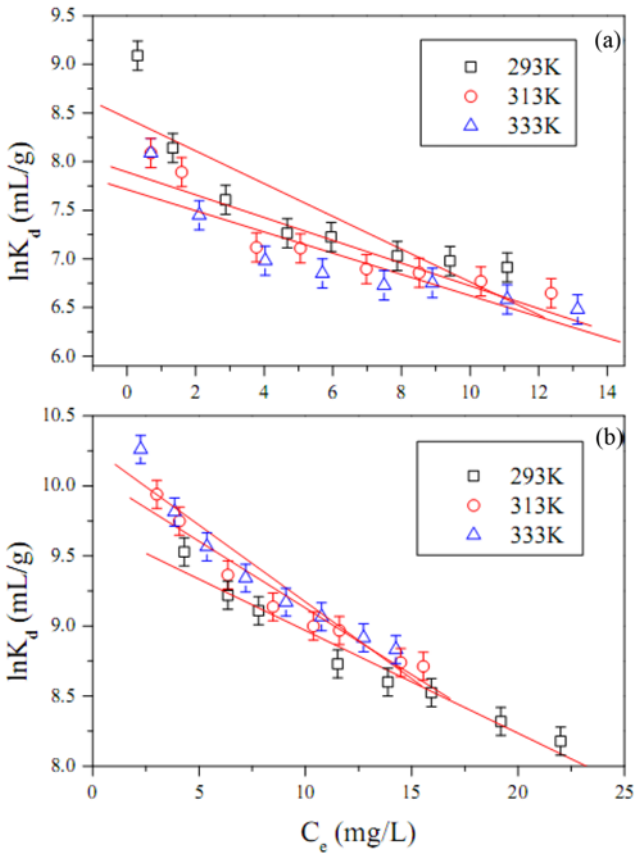

Fig. 11. Linear plots of ln K_d vs. C_e for the adsorption of phenol (a) and 1-naphthol (b) on XC-72 at three different temperatures.

Table 4. The parameters for Langmuir and Freundlich isotherms of Phenol and 1-naphthol at three different temperatures

Phenols	T (K)	Langmuir parameters			Freundlich parameters		
		q_{max} (mg/g)	1/b (mg/L)	R^2	K_F ($mg^{1-n}L^n/g$)	n	R^2
Phenol	293	12.62	2.67	0.93	4.10	2.61	0.98
	313	12.10	4.15	0.93	2.86	2.11	0.96
	333	11.10	4.67	0.92	2.55	2.16	0.98
1-Naphthol	293	83.54	1.38	0.99	47.54	5.80	0.97
	313	99.50	1.49	0.99	52.01	4.80	0.98
	333	104.60	1.47	0.99	54.37	4.72	0.96

The standard entropy change (ΔS^o) is calculated using the following equation:

$$\Delta S^o = -\left(\frac{\partial \Delta G^o}{\partial T}\right)_p \quad (14)$$

The average standard enthalpy change (ΔH^o) is then calculated from the equation:

$$\Delta H^o = \Delta G^o + T\Delta S^o \quad (15)$$

The thermodynamic data calculated by Eqs. (13)-(15) are listed in Table 5. All the samples present a negative standard free energy change (ΔG^o), which indicates that the adsorption reactions are generally a spontaneous process. The positive standard entropy changes (ΔS^o) demonstrate that the degree of freedom increases at the solid-liquid interfaces during the adsorption of phenols on XC-72 and may indicate some changes of the structure in adsorbent [43-45]. An interesting observation is that the average standard enthalpy changes (ΔH^o) are negative for phenol adsorption on XC-72 while positive for 1-naphthol adsorption. The negative ΔH^o values prove that adsorption process of phenol is exothermic, which is sustained by the observation that adsorption of phenol on XC-72 decreases with increasing temperature (Fig. 11(a)). However, the positive ΔH^o values indicate an endothermic adsorption for 1-naphthol, which accounts for the increase in adsorption of 1-naphthol on XC-72 with increasing temperature (Fig. 11(b)).

Table 5. Thermodynamic parameters of phenols adsorption on XC-72

Phenols	T (K)	ΔG (kJ·mol^{-1})	ΔS (J·mol^{-1}·K^{-1})	ΔH (kJ·mol^{-1})
Phenol	293	−5.20	11.45	−1.85
	313	−5.38	11.45	−1.80
	333	−5.66	11.45	−1.85
1-Naphthol	293	−5.54	22.83	1.15
	313	−6.01	22.83	1.14
	333	−6.45	22.83	1.15

7. Competitive Adsorption of Phenol and 1-Naphthol on XC-72

The adsorption isotherms of phenol and 1-naphthol in single or binary system at 293 K are shown in Fig. 12. From Fig. 12, the adsorption of phenol or 1-naphthol decreases in the presence of another one, which indicates that a competitive adsorption process between phenol or 1-naphthol takes place. The results can be explained from the amount of surface sorption sites of adsorbent. The amount of surface sorption sites of XC-72 is a constant value when the adsorbent content is sure. The surface sorption sites of XC-72 are occupied by phenol and 1-naphthol, and then it can lead to the adsorption of phenol and 1-naphthol decrease. The result is similar to the fluoride and phosphate sorption on calcined Mg-Al-CO_3 layered double hydroxides [46].

8. Comparison with other Adsorbents

The adsorption capacity is an important factor because it deter-

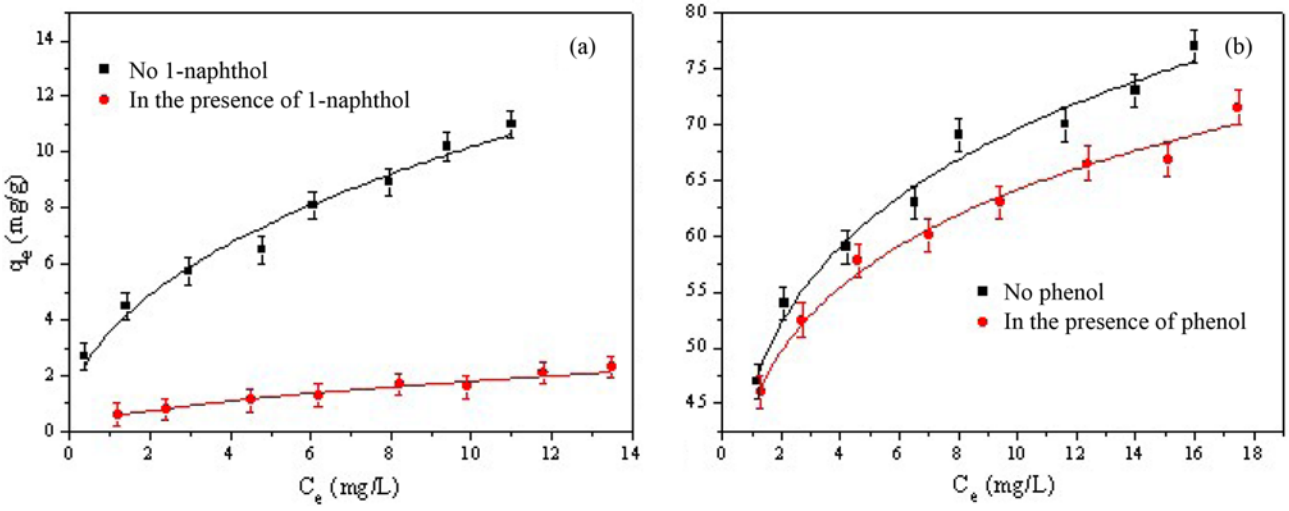

Fig. 12. Adsorption isotherms of phenol (a) and 1-naphthol (b) in the absence and presence of another one. m/V=0.4 g/L, pH=7.0±0.1.

Table 6. Comparison of phenol and 1-naphthol adsorption by various sorbents

Sorbent	q_{max} (mg/g) (phenol)	q_{max} (mg/g) (1-naphthol)	Conditions	References
Carbon nanotubes	14.41	54.35	pH 6.5; T 298 K	[30]
Apatite	9.2	/	pH 6.0; T 298 K	[48]
Zeolite	4.5	/	pH 4.0; T 298 K	[49]
Rice husk	4.51	/	/	[50]
Activated carbon	/	72.08	pH 7.0; T 298 K	[51]
XC-72	12.62	83.54	pH 7.0; T 293 K	This work

mines how much sorbent is needed for quantitative enrichment of the sorbate from a given solution [47]. A comparison of the Langmuir adsorption capacity (q_{max}) of XC-72 carbon investigated in this work with that of other common adsorbents such as carbon nanotubes [30], apatite [48], zeolite [49] rice husk [50] and activated carbon [51] confirms that the adsorption capacity of XC-72 for phenols, especially for 1-naphthol, is higher than that of other adsorbents (Table 6). The results obtained in this paper suggest that XC-72 is an efficient adsorbent for the removal of phenols from large volumes of aqueous solutions.

CONCLUSIONS

The adsorption of phenol and 1-naphthol on XC-72 was investigated by batch technique. Based on the results of this work, the following conclusions can be made:

(1) The adsorption of phenol and 1-naphthol on XC-72 occurred rapidly within the first 3 and 4 h of contact; also the kinetic adsorption of phenol and 1-naphthol on XC-72 can be fitted well by the pseudo-second-order model.

(2) The adsorption of phenol and 1-naphthol on XC-72 is strongly dependent on pH values.

(3) The adsorption isotherms of phenol can be well described by the Freundlich isotherm model, whereas the adsorption isotherms of 1-naphthol are fitted better by the Langmuir isotherm model than the Freundlich isotherm model. The adsorption of phenol or 1-naphthol decreases in the presence of another one due to the competitive adsorption between phenol and 1-naphthol.

(4) The thermodynamic parameters (ΔG^o, ΔS^o and ΔH^o) suggest that the adsorption reactions are spontaneous due to the negative adsorption standard free energy together with positive standard entropy change. The negative ΔH^o values suggest an exothermic adsorption for phenol, while the positive ΔH^o values suggest an endothermic adsorption for 1-naphthol.

(5) XC-72 is suitable adsorbent for the removal of phenol and 1-naphthol from large volumes of aqueous solutions. The findings of this work might have significant implications for the removal of phenols from aqueous solutions with XC-72 in real work.

ACKNOWLEDGEMENT

Financial support from National Natural Science Foundation of China (20971033, 21277039) is acknowledged.

REFERENCES

1. J. J. Yin, R. Chen, Y. S. Ji, C. D. Zhao, G. H. Zhao and H. X. Zhang, *Chem. Eng. J*., **157**, 466 (2010).
2. I. Rodriguez, M. P. Llompart and R. Cela, *J. Chromatogr. A*., **885**, 291 (2000).
3. A. A. Sameer, B. Fawzi and A. A. Leena, *Sep. Purif. Technol*., **33**, 1 (2003).
4. Z. Li, M. Wu, Z. Jiao, B. Bao and S. Lu, *J. Hazard. Mater*., **114**, 111 (2004).
5. D. D. Shao, G. D. Sheng, C. L. Chen, X. K. Wang and M. Nagatsu, *Chemosphere*, **79**, 679 (2010).
6. T. S. Anirudhan, S. S. Sreekumari and C. D. Bringle, *Adsorption*, **15**, 439 (2009).
7. J. Hu, D. D. Shao, C. L. Chen, G. D. Sheng, J. X. Li, X. K. Wang and M. Nagatsu, *J. Phys. Chem. B*., **114**, 6779 (2010).
8. L. J. Kennedy, J. J. Vijaya, K. Kayalvizhi and G. Sekaran, *Chem. Eng. J*., **132**, 279 (2007).
9. M. Ahmaruzzaman and D. K. Sharma, *J. Colloid Interface Sci.*, **287**, 14 (2005).
10. C. L. Chen, X. K. Li, D. L. Zhao, X. L. Tan and X. K. Wang, *Colloids Surf. A*., **302**, 449 (2007).
11. T. S. Anirudhan, S. S. Sreekumari and C. D. Bringle, *Adsorption*, **15**, 439 (2009).
12. J. Lohwacharin, K. Oguma and S .Takizawa, *Water. Res.*, **43**, 3076 (2009).
13. U. Ghosh, *Hum. Ecol. Risk. Assess*., **13**, 276 (2007).
14. J. Yu, W. Du, F. Zhao and B. Zeng, *Electrochim. Acta*, **54**, 984 (2009).
15. D. D. Shao, Z. Q. Jiang and X. K. Wang, *Plasma Process. Polym*., **7**, 552 (2010).
16. C. L. Chen, J. Hu, D. Xu, X. L. Tan, Y. D. Meng and X. K. Wang, *J. Colloid Interface Sci*., **323**, 33 (2008).
17. J. Hu, C. L. Chen, X. X. Zhu and X. K. Wang, *J. Hazard. Mater*., **162**, 1542 (2009).
18. A. M. Bond, W. Miao and C. L. Raston, *Langmuir*, **16**, 6004 (2000).
19. D. D. Shao, Z. Q. Jiang, X. K. Wang, J. X. Li and Y. D. Meng, *J. Phys. Chem. B*., **113**, 860 (2009).
20. C. L. Chen, B. Liang, A. Ogino, X. K. Wang and M. Nagatsu, *J. Phys. Chem. C*., **113**, 7659 (2009).
21. D. D. Shao, Q. H. Fan, J. X. Li, Z. W. Niu, W. S. Wu, Y. X. Chen and X. K. Wang, *Micro. Macro. Material*., **123**, 1 (2009).
22. D. D. Shao, D. Xu, S. Wang, Q. H. Fan, W. Wu, Y. Dong and X. K. Wang, *Sci. China B*., **52**, 362 (2009).
23. X. L. Tan, P. P. Chang, Q. H. Fan, X. Zhou, S. M. Yu, W. S. Wu and X. K. Wang, *Colloids Surf. A*., **328**, 8 (2008).
24. X. L. Tan, Q. H. Fan, X. K. Wang and B. Grambow, *Environ. Sci. Technol*., **43**, 3115 (2009).
25. D. Xu, X. L. Tan, C. L. Chen and X. K. Wang, *J. Hazard. Mater*., **154**, 407 (2008).
26. X. Y. Guo, S. Z. Zhang and X. Q. Shan, *J. Hazard. Mater*., **151**, 134 (2008).
27. Y. Huang, X. Y. Ma, G. Z. Liang and H. X. Yan, *Chem. Eng. J*., **141**, 1 (2008).
28. W. Chen, L. Duan, L. L. Wang and D. Q. Zhu, *Environ. Sci. Technol*., **42**, 6862 (2008).
29. K. Yang, W. Wu, Q. Jing and L. Zhu, *Environ. Sci. Technol*., **42**, 7931 (2008).
30. G. D. Sheng, D. D. Shao, X. M. Ren, X. Q. Wang, J. X. Li, Y. X. Chen and X. K. Wang, *J. Hazard. Mater*., **178**, 505 (2010).
31. L. G. Yan, X. Q. Shan, B. Wen and S. Z. Zhang, *J. Colloid Interface Sci*., **308**, 11 (2007).
32. V. C. Srivastava, M. M. Swamy, I. D. Mall, B. Prasad and I. M. Mishra, *Colloids Surf. A*., **272**, 89 (2006).
33. W. Chen, L. Duan and D. Zhu, *Environ. Sci. Technol*., **41**, 8295 (2007).
34. C. L. Chen, A. Ogino, X. K. Wang and M. Nagatsu, *Appl. Phys. Lett*., **96**, 131504 (2010).
35. C. L. Chen, X. K. Wang and M. Nagatsu, *Environ. Sci. Technol*., **43**, 2362 (2009).

36. Q. H. Fan, X. L. Tan, J. X. Li, X. K. Wang, W. S. Wu and G. Montavon, *Environ. Sci. Technol*., **43**, 5776 (2009).
37. Q. H. Fan, D. D. Shao, J. Hu, C. L. Chen, W. S Wu and X. K. Wang, *Radiochim. Acta*, **97**, 141 (2009).
38. X. L. Tan, X. K. Wang, M. Fang and C. L. Chen, *Colloids Surf. A*., **296**, 109 (2007).
39. B. Pan and B. S. Xing, *Environ. Sci. Technol*., **42**, 9005 (2008).
40. G. X. Zhao, H. X. Zhang, Q. H. Fan, X. M. Ren, J. X. Li, Y. X. Chen and X. K. Wang, *J. Hazard. Mater*., **173**, 661 (2010).
41. S. Mukherjee, S. Kumar, A. K. Misra and M. Fan, *Chem. Eng. J*., **129**, 133 (2007).
42. X. L. Tan, M. Fang, C. L. Chen, S. M. Yu and X. K. Wang, *Carbon*, **46**, 1741 (2008).
43. Z. Z. Chowdhury, S. M. Zain, R. A. Khan and M. S. Islam, *Korean J. Chem. Eng*., **29**, 1 (2012).
44. X. L. Tan, M. Fang and X. K. Wang, *J. Nanosci. Nanotechnol*., **8**, 5624 (2008).
45. G. D. Sheng, J. X. Li, D. D. Shao, J. Hu, C. L. Chen, Y. X. Chen and X. K. Wang, *J. Hazard. Mater*., **178**, 333 (2010).
46. P. Cai, H. Zheng, C. Wang, H. W. Ma, J. C. Hu, Y. B. Pu and P. Liang, *J. Hazard. Mater*., **213**, 100 (2012).
47. A. Stafiej and K. Pyrzynska, *Sep. Purif. Technol*., **58**, 49 (2007).
48. A Bahdod, S. E. Asri, A. Saoiabi, T. Coradin and A. Laghzizil, *Water. Res*., **43**, 313(2009).
49. R. I. Yousef and B. El-eswed, *Colloids Surf. A*., **334**, 92 (2009).
50. M. Ahmaruzzaman and D. K. Sharma, *J. Colloid Interface Sci*., **287**, 14 (2005).
51. M. Anbia and S. E. Moradi, *Korean J. Chem. Eng*., **29**, 743 (2012).